

PHARMACOKINETIC ANALYSIS OF TOPOTECAN AFTER SUPERSELECTIVE OPHTHALMIC ARTERY INFUSION AND PERIOCCULAR ADMINISTRATION IN A PORCINE MODEL

PAULA SCHAIQUEVICH, PhD,* EMILIANO BUITRAGO, BS^c,† ALEJANDRO CECILIANO, MD,‡
ADRIANA C. FANDINO, MD,§ MARCELO ASPREA, DVM,¶ SERGIO SIERRA, MD,‡
DAVID H. ABRAMSON, MD,** GUILLERMO F. BRAMUGLIA, PhD,† GUILLERMO L. CHANTADA, MD††

Purpose: To characterize the vitreous and plasma pharmacokinetics of topotecan after ophthalmic artery infusion (OAI) subsequent to superselective artery catheterization and to compare it with periocular injection (POI).

Methods: The ophthalmic artery of 4 pigs was catheterized and 1 mg of topotecan infused over a period of 30 minutes. The contralateral eye was subsequently used for administering topotecan by POI. Serial vitreous specimens were obtained by microdialysis and plasma samples collected and assayed for total and lactone topotecan.

Results: Maximum total topotecan concentration in the vitreous (median, range) was significantly higher after OAI compared with POI (131.8 ng/mL [112.9–138.7] vs. 13.6 ng/mL [5.5–15.3], respectively; $P < 0.005$). Median vitreous exposure calculated as area under the curve for total topotecan attained after OAI was significantly higher than after POI (299.8 ng·hour/mL [247.6–347.2] and 48.9 ng·hour/mL [11.8–63.4], respectively; $P < 0.05$). The vitreous to plasma exposure ratio was 29 after OAI and 3.4 after POI. Systemic exposure for total topotecan was low after both modalities of administration, with a trend to be lower after OAI compared with POI (10.6 ng·hour/mL [6.8–13.4] vs. 18.7 ng·hour/mL [6.3–21.7]; $P = 0.54$).

Conclusion: Superselective OAI resulted in significantly higher vitreous concentrations and exposure and a trend toward lower systemic exposure than POI.

RETINA X:1–9, 2011

Conservative treatment in retinoblastoma has recently evolved from external-beam radiotherapy to systemic chemotherapy followed by consolidation with focal therapies to avoid the potentially fatal radiation-induced neoplasms.¹ However, eyes with vitreous seeding of tumor cells are difficult to cure with this treatment^{2,3} because intravenously administered chemotherapy fails to effectively reach the vitreous because of its lack of vascularization, the blood–retinal barrier,⁴ and the presence of multidrug-resistance transporters that efflux substrates out of the target cell.^{5,6} In children, further intensifying systemic chemotherapy is not recommended because of unacceptable short- and long-term toxicity, including chemotherapy-induced leukemia.⁷ Therefore, different routes for local chemotherapy administration are

under investigation for the treatment of eyes with advanced disease, in particular those with vitreous seeding, to improve the vitreous drug delivery while minimizing the systemic drug exposure.⁸ These routes of local chemotherapy administration include periocular application,^{9–11} intravitreal injections,^{12,13} and, recently, selective chemotherapy infusion by means of the ophthalmic artery.^{14,15} This technique was initially developed for the administration of melphalan by Yamane et al,¹⁶ by delivering the drug by means of a balloon catheter placed in the internal carotid artery. The balloon was inflated beyond the ophthalmic artery orifice to occlude the carotid artery so that the infused chemotherapy could reach the ophthalmic artery.¹⁶ Abramson et al¹⁴ recently optimized this technique by administering chemotherapy

by means of a superselective arterial catheterization of the ophthalmic artery in a phase I/II study with encouraging results. Because of the promising effectiveness for children with advanced disease, many centers are now using this strategy for treatment of intraocular retinoblastoma.^{17,18} It is presumed that these excellent results are a consequence of a better chemotherapy disposition in the eye concerning other routes of administration, allowing for high concentrations of the drug in the vitreous. However, there are no comparative pharmacokinetic studies supporting its use. Because vitreous pharmacokinetic studies for retinoblastoma in humans are obviously limited by the impossibility of obtaining vitreous specimens, non-tumor-bearing and tumor-bearing animal models (usually rabbits and mice) were traditionally used for these studies. Catheterization of the ophthalmic artery and intraarterial administration of chemotherapy are not feasible in small tumor-bearing animal models and hence finding the adequate model for a pharmacokinetic study of intraarterial chemotherapy is a challenge. We decided to test the feasibility of the porcine model for carrying out a pharmacokinetic study of systemic and vitreous drug exposure after intraarterial chemotherapy administration because its vascular anatomy has been previously characterized and its use for ocular research has been reported.^{19,20} Based on our own previous experience,^{21–23} and preclinical²⁴ and clinical²⁵ evidences of activity against retinoblastoma, we chose topotecan as the candidate drug for the present study. Therefore, the aim of this study was to investigate the vitreous and plasma pharmacokinetics of topotecan after superselective ophthalmic artery infusion (OAI) compared with periocular

injection (POI) in a porcine model as a translational study to support its possible use in retinoblastoma treatment.

Materials and Methods

Animal Studies and Topotecan Administration

Four domestic Landrace pigs (weight 30–45 kg) were used after the approval of the local institutional review board for animal welfare. This study also complies with the tenets of the Association for Research in Vision and Ophthalmology for the use of animals in ophthalmic and vision research.

All animals received an intramuscular injection of 20 mg/kg ketamine in combination with 0.2 mg/kg midazolam and 0.1 mg/kg acepromazine for sedation. General anesthesia was then induced with an intravenous injection of 12 mg/kg thiopental. The animals were maintained under mechanical ventilation with isoflurane 2% and 2 μ g/kg fentanyl and 0.1 mg/kg pancuronium throughout the experiments. Each animal was used in 2 occasions and was randomly allocated to receive 1 of the 2 sequences of drug treatment. One sequence consisted of an OAI of topotecan followed by the pharmacokinetic study. After a washout period of at least 1 week, the same animal underwent a second pharmacokinetic study in which the fellow eye was treated with a POI of the same dose of topotecan or the reverse order. Thus, both eyes from each animal were used for pharmacokinetic analysis, one eye per occasion, and each eye was studied only once.

Periocular injection was carried out injecting 1 mL of topotecan solution (1 mg/mL in 0.9% saline solution) in the subtenon space with a 25-gauge and 1.25-inch needle.

The ophthalmic artery catheterization was carried out in the anesthetized animal under heparin (75 UI/kg) anticoagulation. A 5-French arterial sheath (Johnson & Johnson, Cordis Corp., Miami Lakes, FL) was placed indistinctively in the right or left femoral artery. Afterwards, a 5-F guide catheter (Envoy guide catheter; 5-F MPC, Cordis Corp., Miami Lakes, FL) was placed indistinctively in the right or left femoral artery. Afterward, a 5F guide catheter (Envoy guide catheter, 5F MPC; Cordis) was guided into the common carotid artery that is continued by the external carotid that gives off the maxillary artery in pigs. The angiographic series images were acquired and recorded with a GE Stenoscop C-arm, 9-inch image intensifier. The matrix resolution was of 576 \times 576 pixels, with an acquisition rate of 4 subtracted frames per second. The ophthalmic artery was superselectively catheterized using

*Clinical Pharmacokinetics Unit, CONICET-Hospital de Pediatría JP Garrahan, Buenos Aires, Argentina; †Department of Pharmacology, Faculty of Pharmacy and Biochemistry, University of Buenos Aires, Buenos Aires, Argentina; ‡Interventional Radiology and §Ophthalmology, and ¶Office of Laboratory Animal Care, Department of Laboratory Services, Hospital de Pediatría JP Garrahan, Buenos Aires, Argentina; **Department of Ophthalmic Oncology, Radiotherapy and Surgery, Memorial Sloan-Kettering Center Cancer Center, New York, New York; ††Department of Hematology-Oncology, Hospital de Pediatría JP Garrahan, Buenos Aires, Argentina.

G. F. Bramuglia and G. L. Chantada have equally contributed to the development of this work.

This work was supported by Consejo Nacional de Investigaciones Científicas y Técnicas (PIP Nr 11220090100343), Hospital JP Garrahan, Buenos Aires, Argentina; Fund for Ophthalmic Knowledge (G.L.C. and A.C.F.), New York, New York; and Fundación Natalie D Flexer de Ayuda al Niño con Cáncer (G.L.C. and A.C.F.), Buenos Aires, Argentina.

The authors report no conflicts of interest.

Reprint requests: Guillermo L. Chantada, MD, Department of Hematology-Oncology, Hospital de Pediatría JP Garrahan, Combate de los Pozos 1881, C1245AAL Buenos Aires, Argentina; e-mail: gchantada@yahoo.com

a microcatheter with an outer diameter at the distal tip of 1.2F or 0.4 mm Magic MP (Balt Therapeutics, Montgomery, France). Superselective angiograms were carried out to verify the position of the microcatheter and the ocular vascularization as shown in Figure 1. Topotecan (1 mg in 30 mL of saline) was then delivered in a pulsatile fashion over a period of 30 minutes as described by Abramson et al.¹⁴ Finally, the microcatheter was removed and the procedure for systematic procurement of vitreous and plasma samples started immediately.

Vitreous Sampling Technique

Vitreous samples were collected using the *in vivo* microdialysis technique as previously described.²² This technique allows for serial sampling of the vitreous over an extended period of time allowing to carry out a complete pharmacokinetic profile in a single animal, thus limiting the number of animals used for the study to a minimum.²⁶ Briefly, the principle of the technique consists of the diffusion of topotecan from the vitreous humor through a dialysis membrane inserted in a probe in continuous exposure with the perfusion fluid (phosphate-buffered saline, pH 7.4) delivered at a flow rate of 1 $\mu\text{L}/\text{minute}$ that transports the drug to be collected for posterior drug quantitation. After the ophthalmic artery was catheterized, the microdialysis probe was inserted into the vitreous space through an incision made with a 25-gauge needle and fixed to the animal conjunctiva using 6-0 vicryl sutures. Then, topotecan was infused over a period of 30 minutes and dialysates from the vitreous humor were collected during 30-minute

intervals over a period of 4 hours after topotecan intraarterial administration. At the end of 3 separate experiments, *in vivo* recovery was determined by perfusing the probe with a concentrated topotecan solution (200 ng/mL) and estimating the recovery by the retrodialysis method. The mean recovery value obtained for the probes was 22.8% (± 6.3 SD) and was used to calculate the actual topotecan concentrations in each dialysate vitreous collection.

Sample Schedule and Topotecan Analysis

Arterial blood samples were obtained from the femoral catheter at 0.083, 0.25, 0.50, 0.75, 1.0, 1.5, 2.0, 2.5, 3.0, 3.5, and 4.0 hours after topotecan OAI was finished or after POI. Once collected, blood samples were immediately centrifuged and 50 μL of plasma was treated with 200 μL of cold methanol to precipitate the proteins and stabilize topotecan equilibrium between the lactone and the carboxylate forms.²¹ Finally, all methanolic supernatant extracts and dialysates were stored at -20°C until analysis. Topotecan lactone and carboxylate concentrations were determined by high-performance liquid chromatography coupled with fluorometric detection as previously described and total topotecan (lactone plus carboxylate) was calculated.^{21,23} The assay was previously validated, and the lower limit of quantitation was 1 ng/mL and the intraday and interday precision $<7\%$.^{21,23}

Pharmacokinetic and Statistical Analyses

A two-compartment model was selected to simultaneously fit total topotecan vitreous and plasma concentrations versus time data after OAI. Individual pharmacokinetic parameters were obtained using the ADAPT software, version 5, by means of maximum likelihood estimation method (Biomedical Simulations Resource, Los Angeles, CA).²⁷ Data from 1 animal was better described by a 3-compartment model. However, because of the parsimony principle and the statistical parameters, a 2-compartment model with first-order elimination as shown in Figure 2A was finally selected to describe total topotecan disposition in the vitreous and plasma after ophthalmic artery administration of the dose D . The pharmacokinetic parameters estimated included elimination rate constant (k_c), volume of distribution of the central compartment (V_{pl}), the intercompartment rate constants (k_{cv} , k_{vc}), and the apparent volume of distribution of the vitreous compartment that was fixed to 2 mL²⁸ to reduce the number of degrees of freedom. The area under the total topotecan vitreous and plasma concentrations versus time profile from 0 to 4 hours, a parameter of drug exposure (AUC_{vit} and AUC_{pl} ,



Fig. 1. Representative arteriogram from the left eye of a pig before topotecan administration.

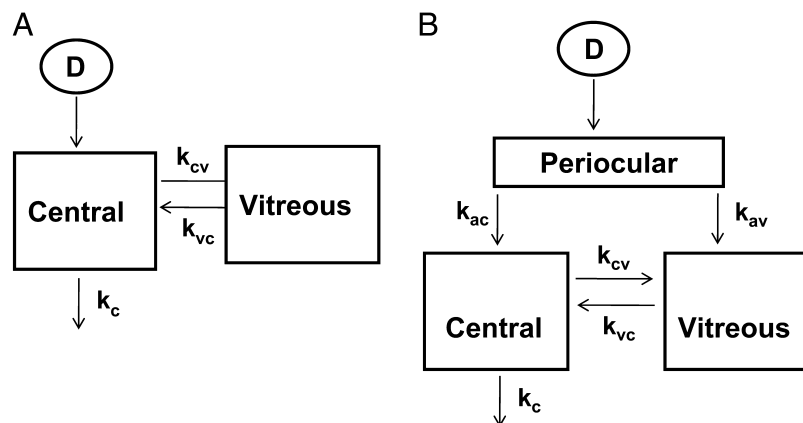


Fig. 2. Pharmacokinetic compartmental model for vitreous and plasma total topotecan after superselective OAI (A) and POI (B). The pharmacokinetic parameters estimated included elimination rate constant (k_c), volume of distribution of the central compartment (V_{pl}), the intercompartment rate constants (k_{cv} , k_{vc}), and the apparent volume of distribution of the vitreous compartment that was fixed to 2 mL.

respectively), was calculated by integration of the simulated concentration–time data from model estimates. The maximum concentration (C_{max}) was obtained from observed data.

A 2-compartment model was also selected to describe total topotecan in the vitreous and plasma compartments after POI, as presented in Figure 2B, and pharmacokinetic parameters were estimated as previously discussed including k_{ac} and k_{av} as the absorption rate constants from the periocular space where the dose D is given to the central and vitreous compartments, respectively. An apparent volume of distribution of the central compartment was considered as V_{pl}/F where F is the bioavailability fraction.

Because of inherent limitations in the microdialysis technique for vitreous sampling, interconversion between lactone and carboxylate topotecan occurs during each interval of sample collection. Therefore, total topotecan was considered for pharmacokinetic modeling in vitreous samples simultaneously with total plasma concentrations. Topotecan lactone concentrations were, however, estimated in plasma samples because they were collected serially and almost instantly by arterial sampling and immediately preventing from interconversion. Thus, lactone and carboxylate topotecan concentrations versus time data after OAI and POI were modeled separately to calculate systemic exposure to the lactone form as the active pharmacologic moiety. In these cases, a two-compartment model was used to simultaneously fit plasma lactone and carboxylate topotecan.

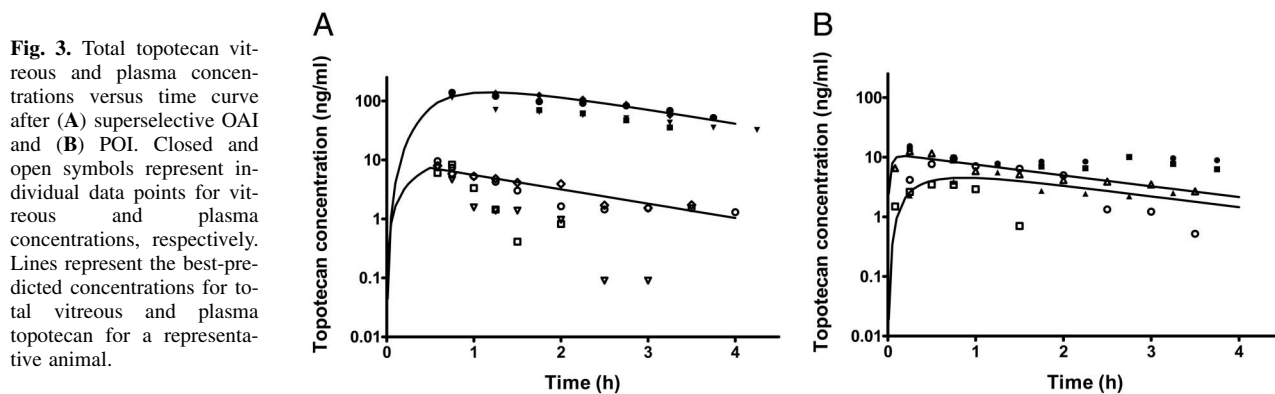
Finally, the pharmacokinetic parameters were compared between groups by means of a paired t -test and examined for significance at a level of 0.05.

Results

A total of 4 eyes from 4 animals were used to study topotecan pharmacokinetics after superselective OAI.

All 4 animals underwent successful ophthalmic artery catheterization that enabled the superselective administration of topotecan as shown in a representative angiogram (Figure 1). As previously described, each animal underwent a second pharmacokinetic study after a washout period, in which the fellow untreated eye was given a POI of topotecan. However, 1 animal died during the anesthetic procedure in the study of POI; therefore, 3 eyes of 3 animals were evaluated in this group. The disposition of total topotecan in plasma and the vitreous humor of the injected eye after OAI and POI was described by a 2-compartment model as represented in Figure 2, A and B, respectively. The model adequately fitted the concentration versus time data after OAI reflected by the visual inspection plots as shown in Figure 3A and statistical parameters. Topotecan pharmacokinetic parameters after both routes of drug administration are presented in Table 1. Although the two-compartment model was the best approach to simultaneously model the plasma and vitreous total topotecan concentration after topotecan POI, it presents a limitation in the estimation of the pharmacokinetic parameters and it might lead to a probable overestimation of the vitreous total topotecan AUC after this modality as shown in Figure 3B.

The observed vitreous and plasma total topotecan C_{max} values were evident at the end of OAI and the median (range) values were 131.8 ng/mL (112.9–138.7) and 8.1 ng/mL (7.4–9.5), respectively. After POI, total topotecan vitreous and plasma median (range) C_{max} values were 13.6 ng/mL (5.5–15.3) and 9.5 ng/mL (3.5–12.6), respectively. A significant increase was observed in vitreous total topotecan C_{max} after OAI when compared with POI ($P = 0.002$) as shown in Table 2. No significant difference was found when comparing total topotecan C_{max} in plasma between both routes of administration (data not shown, $P = 0.97$). Together, these results indicate that



median total topotecan vitreous C_{max} was significantly higher after OAI compared with the results obtained after POI. Thus, this modality was also associated to lower but not significant maximum plasma concentration ($P = 0.97$).

Median (range) total topotecan AUC in vitreous was significantly higher after OAI compared with POI, 299.8 ng·hour/mL (255.2–347.2) and 48.9 ng·hour/mL (11.8–63.4), respectively ($P = 0.02$). These results show that the median vitreous exposure to total topotecan after OAI was about 6-fold the value obtained after POI ($AUC_{vit,OAI}/AUC_{vit,POI}$; Table 2). However, there was no significant difference in systemic AUC for total or lactone topotecan between the two routes of administration ($P = 0.54$; Table 2).

As presented in Table 2, the median vitreous to plasma topotecan exposure ratio (AUC_{vit}/AUC_{pl}) after OAI was 29 implying that vitreous exposure to total topotecan was 29 times greater in the vitreous humor compared with systemic exposure, whereas it was only 3.4 after POI. Thus, the vitreous to plasma exposure ratio was almost nine times higher after OAI compared with the POI.

The results obtained in a representative animal comparing total topotecan ocular and systemic disposition after both local routes of topotecan administration are shown in Figure 4, A and B, respectively. The vitreous exposure for this animal

after OAI was 347.2 ng·hour/mL and after POI 11.8 ng·hour/mL. Thus, the vitreous exposure ratio between these two routes of local topotecan administration ($AUC_{vit,OAI}/AUC_{vit,POI}$) was 29.4. On the contrary, total topotecan systemic exposure was 13.2 ng·hour/mL after OAI and 21.7 ng·hour/mL after POI, resulting in a ratio of 0.6. Hence, a significant increase in total topotecan vitreous exposure is shown after OAI compared with the same dose given by POI.

Finally, we observed that the median (range) total topotecan level in the vitreous was 35.8 ng/mL (16.9–42.4) after 4 hours of OAI, and the levels were above 14 ng/mL up to 6 hours after the infusion in 2 animals. On the contrary, after 4 hours of POI, the median total topotecan level in the vitreous of the treated eyes was only 4.2 ng/mL (1.5–5.7); however, this difference was not significant ($P = 0.08$).

Discussion

Despite superselective OAI for local administration of chemotherapy to the eye being currently evaluated for the treatment of children with retinoblastoma, this work represents, to our knowledge, the first pharmacokinetic analysis reported for a chemotherapy drug administered by this technique. In addition, this is the first report evaluating and comparing topotecan

Table 1. Pharmacokinetic Parameters Obtained After OAI and POI of Topotecan (1 mg)

Pharmacokinetic Parameter	OAI	POI
k_{ac} h ⁻¹	—	8.6 (5.3–24.7)
k_{av} h ⁻¹	—	0.59 (0.42–0.75)
V_{pl}/F (L)	51.2 (32.6–60.0)	6.3 (1.5–27.0)
k_{cv} h ⁻¹	0.0017 (0.0012–0.0018)	2.6 (0.18–9.19)
k_{vc} h ⁻¹	1.36 (0.57–1.89)	2.65 (1.57–3.39)
k_c h ⁻¹	1.15 (0.54–1.92)	0.95 (0.007–3.0)

Data are shown as median (range). k_{ac} , absorption rate constant to the central compartment; k_{av} , absorption rate constant to the vitreous compartment; V_{pl}/F , volume of distribution of the central compartment. After OAI, $F = 1$; k_{cv} and k_{vc} , intercompartment rate constants; k_c , elimination rate constant; the apparent volume of distribution of the vitreous compartment was fixed to 2 mL.

Table 2. Plasma and Vitreous Exposure for Total and Lactone Topotecan After Superselective OAI and POI of Topotecan (1 mg) in the Pig

	Vitreous		Plasma			AUC Ratio		
	AUC _{vit}	C _{max, vit}	AUC _{pl, T}	AUC _{pl, L}	AUC _{vit} /AUC _{pl}	AUC _{vit, OAI} /AUC _{vit, POI}	AUC _{pl, TOAI} /AUC _{pl, TPOI} *	AUC _{pl, LOAI} /AUC _{pl, LPOI} †
OAI	299.8 (247.6–347.2)	131.8 (112.9–138.7)	10.6 (6.8–13.4)	3.8 (2.0–6.9)	29	6.1	0.6	0.5
POI	48.9‡ (11.8–63.4)	13.6§ (5.5–15.3)	18.7¶ (6.3–21.7)	7.4¶ (3.1–9.3)	3.4	—	—	—

Values are shown as median (range). Topotecan exposure is presented as AUC (ng·hour/mL) and C_{max} (ng/mL). AUC_{vit}, area under the vitreous concentration–time curve for total topotecan; C_{max, vit}, total topotecan maximum concentration in vitreous; AUC_{pl, T}, area under the plasma concentration–time curve for total topotecan; AUC_{pl, L}, area under the plasma concentration–time curve for lactone topotecan; AUC_{vit}/AUC_{pl}, ratio of total topotecan exposure in vitreous and plasma; AUC_{vit, OAI}/AUC_{vit, POI}, ratio of total topotecan exposure in vitreous after OAI and POI, respectively.

*Ratio of topotecan exposure in plasma measured as total and lactone after OAI.

†Ratio of topotecan exposure in plasma measured as total and lactone after POI.

‡P < 0.05 compared with AUC_{vit} after OAI.

§P < 0.005 compared with C_{max, vit} after OAI.

¶P > 0.05 compared with AUC_{pl} after OAI.

systemic and vitreous exposure using this modality with another local route of chemotherapy administration for retinoblastoma currently used in the clinical setting such as the periocular administration.

The use of intraarterial chemotherapy for the treatment of retinoblastoma received enormous attention after the encouraging results reported by Abramson et al¹⁴ in 2008 with their technique for superselective catheterization. The authors reported excellent clinical results in terms of efficacy and toxicity after melphalan monotherapy, especially for newly diagnosed patients with unilateral disease.¹⁴ They subsequently reported a more limited series of children with refractory retinoblastoma that received topotecan or topotecan plus carboplatin.¹⁵ However, preclinical pharmacokinetic data are still lacking and it is of vital importance to determine whether the antineoplastic drug is able to reach the target site, especially the vitreous and if the achieved levels would be sufficient to exert the pharmacologic effect. In addition, our results suggest that after administering the same dose (1 mg),

topotecan penetrated into the vitreous cavity with significantly greater efficiency after the superselective OAI than after POI, with a trend toward a decrease in systemic exposure. When chemotherapy is administered by POI, the physical barriers including the sclera and the retinal pigment epithelium play a critical role in limiting its diffusion into the vitreous cavity.²⁹ In addition, rapid clearance from the orbit to the systemic circulation and the presence of drug transporters also restrict the drug penetration and disposition into the vitreous.^{5,21} When chemotherapy is administered by OAI, some of these barriers, such as the scleral, are avoided and they are not a limitation for the disposition of the drug to the vitreous.

The more advantageous pharmacokinetic profile of topotecan after OAI compared with POI is based on the following observations:

1. Significantly higher vitreous levels measured as C_{max}: In the present study, we observed that the median vitreous C_{max} after OAI (C_{max, vit} = 131.8 ng/mL) was

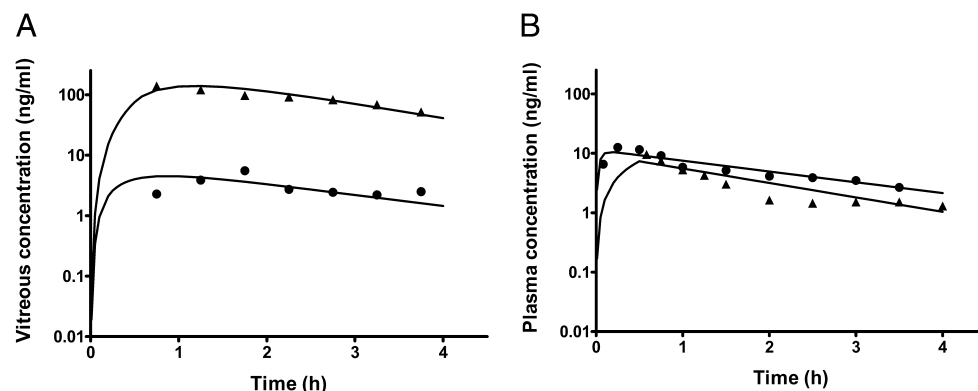


Fig. 4. Total topotecan (A) vitreous and (B) plasma concentrations versus time curve after (▲) superselective OAI and (●) POI for a representative animal. Symbols represent individual data points and lines represent the best-predicted concentrations for total topotecan.

almost 10 times greater than after POI ($C_{\max, \text{vit}} = 13.6$ ng/mL) implying a significant difference ($P < 0.005$). Interestingly, these high and sustained vitreous levels with potential activity against retinoblastoma were detected up to 4 hours of topotecan superselective OAI, with a median value of 35.8 ng/mL. Levels >14 ng/mL are necessary for an antitumor effect according to *in vitro* data.²⁴ This concentration was only achieved at the peak after intravenous or periocular topotecan administration in our previous work in the rabbit model and barely achieved in the present model.²¹ In both models of POI, topotecan levels rapidly decayed to concentrations less than the predefined threshold level of 14 ng/mL.²¹ Therefore, potentially pharmacologic active levels were only achieved at the maximum concentration after POI of topotecan in the rabbits and in the present porcine model, as opposed to OAI where levels >14 ng/mL were seen at least up to 4 hours of administration.

2. Significantly higher vitreous exposure using the concentration versus time curve: For many antineoplastic drugs exerting their antitumor effect in the S phase, like topotecan, the drug exposure expressed as AUC is a representative pharmacokinetic parameter that correlates with the antitumor activity and systemic adverse effects.³⁰ Vitreous topotecan AUC_{vit} was significantly higher after OAI than after POI, showing a median value of 299.8 ng·hour/mL compared with 48.9 ng·hour/mL, respectively. In addition, the relative median ratio of vitreous to plasma exposure ($AUC_{\text{vit}}/AUC_{\text{pl}}$) for total topotecan was 29 after OAI and 3.4 after POI. The lower AUC ratio after POI is an indicator of the limitations for the transscleral penetration of topotecan that result in lower vitreous exposure. The favorable drug disposition in the vitreous after OAI results from avoiding the scleral barrier and the drug loss at the site of POI because of the orbital clearance. Because topotecan systemic exposure was low, it is unlikely that the fraction of drug absorbed from the systemic circulation could contribute to relevant vitreous exposure after OAI. Interestingly, the ratio of vitreous to plasma total topotecan exposure after POI was higher in the porcine model compared with our previous results in rabbits (3.4 vs. 0.2, respectively).²¹ At least two factors should be considered for the interpretation of these findings: First, differences in the ocular vasculature including collateral arteries and in the ocular anatomy including scleral thickness and the permeability through the retinal pigment epithelium may lead to differences in drug penetration from the site of POI to the vitreous when comparing between models.³¹ Second, different animal size will probably affect the apparent topotecan volume of distribution. In this sense, a lower systemic

exposure compared with what the rabbit model would have predicted was also found by our group in a child receiving periocular topotecan, which was also attributed to differences in the volume of distribution.⁹

Finally, despite using the microdialysis technique for serial vitreous sampling that allowed for a complete pharmacokinetic study comparable with the use of 27 animals if a single sample was taken by vitreous puncture by triplicates at each time point, we could only study 3 eyes in the POI group as 1 animal died during the surgical procedure. So, there may also be a limitation in the calculation of the vitreous exposure in this group.

3. Low systemic exposure: Both modalities were associated with relatively low systemic exposure to topotecan. Topotecan systemic exposure after OAI was lower than after POI without reaching statistical significance. Interestingly, topotecan lactone systemic exposure was <10 ng·hour/mL after both routes of drug administration, which is substantially lower than the reported value of 180 ng·hour/mL to produce severe hematopoietic toxicity in humans.³⁰

Another feature favoring the use of intraarterial topotecan is its low variability observed in vitreous exposure because the coefficient of variation of AUC_{vit} was only 18%. Therefore, relatively predictable drug levels were found at each time interval, which also allowed us to limit the number of animals used in the study.

However, our data have some limitations related to the model used. Because it is impossible to obtain serial dosages of topotecan in other ocular tissues without involving an unacceptable number of animals, our data are limited to the concentrations in the vitreous. Drug levels at other ocular tissues and retinal tumors may be of clinical relevance. However, in the clinical situation, vitreous concentrations of chemotherapy may be higher because of the disruption of the blood–retinal barrier caused by the tumor.³² In addition, also in a hypothetical clinical scenario, both modalities would be applied by repeated applications and there might be differences in the pharmacokinetics in subsequent cycles. However, vitreous pharmacokinetic studies cannot be repeated in the same eye because the disruption in the eye anatomy caused by repeated vitreous punctures may alter the drug disposition to the vitreous.³³ In general, after repeated drug administration, the level of drug accumulation will depend on the frequency and the pharmacokinetics of the drug. However, based on the pharmacokinetic parameter models obtained for each studied animal after POI and OAI administrations and the derived simulated concentrations in vitreous, no accumulation may be expected after repeated drug

administration in the present animal model. Another point to be considered is that vascular damage after repeated intraarterial injections and orbital fibrosis after repeated periocular administrations may also affect the drug disposition to the vitreous.

The present pharmacokinetic study was not designed to compare the toxicity of both modalities. Our results may be used as a background for further clinical studies in children with retinoblastoma, which might be carried out to estimate the efficacy and the maximum tolerated dose and dose-limiting toxicity of each modality. Despite not being a tumor-bearing model, the porcine model is validated to conduct eye vascular and scleral permeability experiments^{20,34} because of its anatomical and physiologic similarities with humans. One major advantage is the size of the animal that allowed us to develop and optimize OAI of topotecan for pharmacokinetic evaluation. Although the superselective catheterization is possible in this model, there are anatomical differences between the vasculature of the porcine eye and the human eye.²⁰ In particular, the ophthalmic artery in the pig is a continuity of the external carotid, whereas in humans it arises from the internal carotid. Differences in collateral branches and the existence of collateral retinal blood vessels may also lead to differences in drug disposition.

In conclusion, superselective OAI of topotecan into the ophthalmic artery results in significantly higher vitreous exposure compared with POI with lower systemic exposure. This favorable pharmacokinetic profile of the drug led to potentially active pharmacologic concentrations up to at least 4 hours of administration.

Key words: ophthalmic artery infusion, pharmacokinetics, porcine model, retinoblastoma, topotecan.

Acknowledgments

The authors thank Jose Lipsich for the first steps in implementing the ophthalmic artery superselective catheterization technique and Mariela Cabezas for technical assistance. Gustavo Williams is acknowledged for his general assistance with the animal care and experiments, and Dr. Javier Opezzo for the design and construction of the microdialysis probes. Finally, the authors also thank Dr. Eduardo Lagomarsino for drug preparation, and Drs. Christian Hocht, Julieta Dominguez, and Ana Torbidoni for their technical support.

References

1. Abramson DH, Scheffer AC. Update on retinoblastoma. *Retina* 2004;24:828–848.

2. Shields CL, Honavar SG, Shields JA et al. Factors predictive of recurrence of retinal tumors, vitreous seeds, and subretinal seeds following chemoreduction for retinoblastoma. *Arch Ophthalmol* 2002;120:460–464.
3. Gunduz K, Gunalp I, Yalcindag N, et al. Causes of chemoreduction failure in retinoblastoma and analysis of associated factors leading to eventual treatment with external beam radiotherapy and enucleation. *Ophthalmology* 2004;111:1917–1924.
4. Gaudana R, Jwala J, Boddu SH, Mitra AK. Recent perspectives in ocular drug delivery. *Pharm Res* 2009;26:1197–1216.
5. Mannerman E, Vellonen KS, Urtti A. Drug transport in corneal epithelium and blood-retina barrier: emerging role of transporters in ocular pharmacokinetics. *Adv Drug Deliv Rev* 2006;58(11):1136–1163.
6. Wilson MW, Fraga CH, Fuller CE, et al. Immunohistochemical detection of multidrug-resistant protein expression in retinoblastoma treated by primary enucleation. *Invest Ophthalmol Vis Sci* 2006;47:1269–1273.
7. Gombos DS, Hungerford J, Abramson DH, et al. Secondary acute myelogenous leukemia in patients with retinoblastoma: is chemotherapy a factor? *Ophthalmology* 2007;114:1378–1383.
8. Meadows AT, Chintagumpala M, Dunkel IJ, et al. Children's oncology group trials for retinoblastoma. In: Singh A, Damato B, Peter J, Murphree AL, Perry JD, eds. *Essentials of Ophthalmic Oncology*. Thorofare, NJ: SLACK Incorporated; 2009:204–205.
9. Chantada GL, Fandino AC, Carcaboso AM, et al. A phase I study of periocular topotecan in children with intraocular retinoblastoma. *Invest Ophthalmol Vis Sci* 2009;50:1492–1496.
10. Pontes de Carvalho RA, Krausse ML, Murphree AL, et al. Delivery from episcleral explants. *Invest Ophthalmol Vis Sci* 2006;47:4532–4539.
11. Abramson DH, Frank CM, Dunkel IJ. A phase I/II study of subconjunctival carboplatin for intraocular retinoblastoma. *Ophthalmology* 1999;106:1947–1950.
12. Kaneko A, Suzuki S. Eye-preservation treatment of retinoblastoma with vitreous seeding. *Jpn J Clin Oncol* 2003;33:601–607.
13. Chevez-Barrios P, Chintagumpala M, Mieler W, et al. Response of retinoblastoma with vitreous tumor seeding to adenovirus-mediated delivery of thymidine kinase followed by ganciclovir. *J Clin Oncol* 2005;23:7927–7935.
14. Abramson DH, Dunkel IJ, Brodie SE, et al. A phase I/II study of direct intraarterial (ophthalmic artery) chemotherapy with melphalan for intraocular retinoblastoma initial results. *Ophthalmology* 2008;115:1398–1404, 1404.e1391.
15. Abramson DH, Dunkel IJ, Brodie SE, et al. Superselective ophthalmic artery chemotherapy as primary treatment for retinoblastoma (chemosurgery). *Ophthalmology* 2010;117:1623–1629.
16. Yamane T, Kaneko A, Mohri M. The technique of ophthalmic arterial infusion therapy for patients with intraocular retinoblastoma. *Int J Clin Oncol* 2004;9:69–73.
17. Shields CL, Ramasubramanian A, Rosenwasser R, Shields JA. Superselective catheterization of the ophthalmic artery for intraarterial chemotherapy for retinoblastoma. *Retina* 2009;29:1207–1209.
18. Balmer A, Munier F, Zografos L. New strategies in pediatric ophthalmic oncology [in French]. *Rev Med Suisse* 2008;4:139–143.
19. Dondelinger RF, Ghysels MP, Brisbois D, et al. Relevant radiological anatomy of the pig as a training model in interventional radiology. *Eur Radiol* 1998;8:1254–1273.

20. Moren H, Undren P, Gesslein B, et al. The porcine retinal vasculature accessed using an endovascular approach: a new experimental model for retinal ischemia. *Invest Ophthalmol Vis Sci* 2009;50:5504–5510.
21. Carcaboso AM, Bramuglia GF, Chantada GL, et al. Topotecan vitreous levels after periocular or intravenous delivery in rabbits: an alternative for retinoblastoma chemotherapy. *Invest Ophthalmol Vis Sci* 2007;48:3761–3767.
22. Carcaboso AM, Chiappetta DA, Opezzo JA, et al. Episcleral implants for topotecan delivery to the posterior segment of the eye. *Invest Ophthalmol Vis Sci* 2010;51:2126–2134.
23. Buitrago E, Hocht C, Chantada G, et al. Pharmacokinetic analysis of topotecan after intravitreal injection. Implications for retinoblastoma treatment. *Exp Eye Res* 2010;91:9–14.
24. Laurie NA, Gray JK, Zhang J, et al. Topotecan combination chemotherapy in two new rodent models of retinoblastoma. *Clin Cancer Res* 2005;11:7569–7578.
25. Chantada GL, Fandino AC, Casak SJ, et al. Activity of topotecan in retinoblastoma. *Ophthalmic Genet* 2004;25:37–43.
26. Hocht C, Opezzo JA, Taira CA. Microdialysis in drug discovery. *Curr Drug Discov Technol* 2004;1:269–285.
27. D'Argenio DZ, Schumitzky A. ADAPT II User's Guide: Pharmacokinetic/Pharmacodynamic Systems Analysis Software. Los Angeles: Biomedical Simulations Resource; 2006.
28. Shafiee A, McIntire GL, Sidebotham LC, Ward KW. Experimental determination and allometric prediction of vitreous volume, and retina and lens weights in Gottingen minipigs. *Vet Ophthalmol* 2008;11:193–196.
29. Ranta VP, Mannermaa E, Lummeppo K, et al. Barrier analysis of periocular drug delivery to the posterior segment. *J Control Release* 2010;148:42–48.
30. Santana VM, Zamboni WC, Kirstein MN, et al. A pilot study of protracted topotecan dosing using a pharmacokinetically guided dosing approach in children with solid tumors. *Clin Cancer Res* 2003;9:633–640.
31. Pitkanen L, Ranta VP, Moilanen H, Urtti A. Permeability of retinal pigment epithelium: effects of permeant molecular weight and lipophilicity. *Invest Ophthalmol Vis Sci* 2005;46:641–646.
32. Wilson TW, Chan HS, Moselhy GM, et al. Penetration of chemotherapy into vitreous is increased by cryotherapy and cyclosporine in rabbits. *Arch Ophthalmol* 1996;114:1390–1395.
33. Dias CS, Mitra AK. Posterior segment ocular pharmacokinetics using microdialysis in a conscious rabbit model. *Invest Ophthalmol Vis Sci* 2003;44:300–305.
34. Olsen TW, Sanderson S, Feng X, Hubbard WC. Porcine sclera: thickness and surface area. *Invest Ophthalmol Vis Sci* 2002;43:2529–2532.